World Academy of Science, Engineering and Technology
International Journal of Materials and Metallurgical Engineering
Vol:14, No:1, 2020

Sustainable Hydrogel Nanocomposites Based on Grafted Chitosan and Clay for Effective Adsorption of Cationic Dye

H. Ferfera-Harrar, T. Benhalima, D. Lerari

***Abstract*—**Contamination of water, due to the discharge of untreated industrial wastewaters into the ecosystem, has become a serious problem for many countries. In this study, bioadsorbents based on chitosan-g-poly(acrylamide) and montmorillonite (MMt) clay (CTS-g-PAAm/MMt) hydrogel nanocomposites were prepared via free-radical grafting copolymerization and crosslinking of acrylamide monomer (AAm) onto natural polysaccharide chitosan (CTS) as backbone, in presence of various contents of MMt clay as nanofiller. Then, they were hydrolyzed to obtain highly functionalized pH-sensitive nanomaterials with uppermost swelling properties. Their structure characterization was conducted by X-Ray Diffraction (XRD) and Scanning Electron Microscopy (SEM) analyses. The adsorption performances of the developed nanohybrids were examined for removal of methylene blue (MB) cationic dye from aqueous solutions. The factors affecting the removal of MB, such as clay content, pH medium, adsorbent dose, initial dye concentration and temperature were explored. The adsorption process was found to be highly pH dependent. From adsorption kinetic results, the prepared adsorbents showed remarkable adsorption capacity and fast adsorption rate, mainly more than 88% of MB removal efficiency was reached after 50 min in 200 mg L^{-1} of dye solution. In addition, the incorporating of various content of clay has enhanced adsorption capacity of CTS-g-PAAm matrix from 1685 to a highest value of 1749 mg g^{-1} for the optimized nanocomposite containing 2 wt.% of MMt. The experimental kinetic data were well described by the pseudo-second-order model, while the equilibrium data were represented perfectly by Langmuir isotherm model. The maximum Langmuir equilibrium adsorption capacity (q_m) was found to increase from 2173 mg g^{-1} until 2221 mg g^{-1} by adding 2 wt.% of clay nanofiller. Thermodynamic parameters revealed the spontaneous and endothermic nature of the process. In addition, the reusability study revealed that these bioadsorbents could be well regenerated with desorption efficiency overhead 87% and without any obvious decrease of removal efficiency as compared to starting ones even after four consecutive adsorption/desorption cycles, which exceeded 64%. These results suggest that the optimized nanocomposites are promising as low cost bioadsorbents.

***Keywords*—**Chitosan, clay, dye adsorption, hydrogels nanocomposites.

H. Ferfera-Harrar is with the Department of Macromolecular Chemistry, University of Sciences and Technology Houari Boumediene USTHB, 16111, Algiers, Algeria (e-mail: harrarhafida@ yahoo.fr).

T. Benhalima is with the Chemistry Faculty, University of Sciences and Technology Houari Boumediene USTHB, 16111, Algiers, Algeria (e-mail: tayeb4647@yahoo.fr).

D. Lerari is with the Institution of Centre de Recherche Scientifique et Technique en Analyses Physico-chimiques(CRAPC), BP384, Bou-Ismail, RP 42004, Tipaza, Algeria (e-mail: lerari_zinai@yahoo.fr.

I. Introduction

CONTAMINATION of water by dyes and toxic metallic ions pollutants due to discharge of industrial wastewaters into the ecosystem, is a very serious environmental problem that has become a growing concern to ecologists and civilians [1]. Many industrial fields such as textile, cosmetic, papermaking and printing, rubber, and food processing produce extensive dying effluents. These dyes show harmful effects on living organisms for even short periods of exposure. It is thus very important to remove dye from wastewater.

The removal of dyes from aqueous environments has been done by means of many technologies, such as adsorption, ion exchange and membrane filtration [2]-[4]. However, adsorption using adsorbent materials is the most popular and effective process due to the ease of operation and economical value.

Regarding the environmental impact and the economic viability, design of eco-friendly and low-cost adsorbents has engrossed much interest. Various adsorbents materials have been adapted. These include agricultural and industrial solid wastes, biomass, inorganic (clays, zeolites, metal oxides), polymers and their hybrids materials [5], [6]. However, some drawbacks, including slow rate adsorption, low capacity, and/ or poor selectivity, limit their practical applications.

Natural polymers are widely applied to prepare hydrogels adsorbents due to their unique advantages: abundance of raw material, safety, biocompatibility, and biodegradability.

Hydrogels are three-dimensional polymeric networks that retain huge quantity of water within their structures. They have been used in various applications, mainly in biomedical and environmental fields owing to their distinctive characteristics such as hydrophilicity, swelling ability, functionality, adsorption capacity and ease of preparation [7], [8].

Polysaccharides-based hydrogels are immerging sustainable materials used as low-cost adsorbents, which have exposed the hypernym functioning in removal of wide range of pollutants containing organic dyes and metal ions. Additionally, their chemical modifications by grafting on the biopolymer backbones during the synthesis of hydrogels help to customize them to respond to external stimuli such as temperature and pH that are an added advantage for wastewater treatment. Among them, CTS, the second most plentiful natural polysaccharide next to cellulose, has been widely investigated (pure or combined natural/synthetic polymers) for biomedical and wastewater treatment (removal of toxic ion metals and

dyes). Also, the reactive NH_2 and OH groups of CTS were convenient for grafting-copolymerization of various hydrophilic monomers like acrylamide (AAm) for improving its properties [9], [10].

Clays were widely used as inorganic nanofiller to elaborate hydrogels nanocomposites due to their availability, non-toxicity, low-cost and hydrophilic nature. Among them, MMt, layered silicate with exchangeable cations and reactive OH groups, is the most used owing to its high in plane strength, stiffness, and high-aspect ratio. The incorporation of clay into polymer network was frequently found to improve the properties of the corresponding hybrids hydrogels materials such as swelling and adsorption capacities, and thus, reduced their production cost [11], [12].

In our previous papers, the studies have been focused on designing adsorbents of CMC-based hydrogels composites beads for the removal of a cationic dye MB selected as the representative dye model [13]-[15].

In the current work, we report on the application of the elaborated hydrogels nanocomposites comprising cross-linked CTS-graft-poly(AAm) as matrix and MMt as nanofiller, in the adsorption of MB from aqueous solutions. It is planned to elaborate nanomaterials with high swelling and retention capacities to trap pollutants from wastewater. Structural and morphological characterizations were performed by XRD and SEM analyses, respectively. The effect of clay loading on adsorption performances was systematically studied with the aim to inspect whether these hydrogels are able to be used in water treatment applications.

II. Experimental Section

A. Materials

CTS with 75% deacetylated, medium molecular weight, and viscosity 200-800 cps was purchased from Aldrich. Acrylamide (AAm), Potassium persulfate (KPS) and N,N'-methylenebisacrylamide (MBA), and all other chemical products of analytical grade were used as received without further purification. The clay MMt of size fraction < 2µm was extracted from bentonite, which was supplied by ENOF Chemical Ltd company in Algeria, and then homoionized with sodium ions [16]. Doubly distilled water was used for synthesis and adsorption studies.

B. Synthesis of Hydrogel Nanocomposites

Hydrogels nanocomposites with different clay contents denoted CTS-g-PAAm/MMt were prepared in aqueous solution at 60 °C according to the standard procedure described in our earlier study [12]. Briefly, CTS was dissolved in 30 mL of acetic acid solution (1% v/v) into three-neck flask, equipped with a reflux condenser, a funnel, a nitrogen flux, and a magnetic stirrer. The flask was placed in bath at 60°C for 30 min and subsequently the KPS was added to the mixture and gently stirred for 15 min to generate radicals. Simultaneously, a suspension of required amount of MMt was prepared under vigorous mechanical stirring for 24 h, ultrasonically treated for 30 min, and then was added the solution of AAm and MBA into the funnel and degassed for 15 min, and subsequently introduced into the flask. After 3h of reaction polymerization, the resulting hydrogel was neutralized, extensively washed with water, dehydrated in excess of ethanol, and then dried in the oven. Apart from the omission of clay, the hydrogel matrix CTS-g-PAAm was prepared according to the same procedure.

Finally, the nanomaterials were hydrolyzed at 95°C for 2h in alkaline solution. During the hydrolysis, the ammonia evolves and carboxamide groups of PAAm are converted to carboxylate ions (COO-). Therefore, the structure of the hydrolyzed hydrogel comprised the functional groups of amide $COONH_2$, amine NH_2, and carboxylate COO-. A schematic illustration of the formation mechanism is shown in Fig. 1. Persulfate ions ($S_2O_8^{2-}$) decompose under heating, generate sulfate anion radicals ($SO_4^{\bullet-}$), and then produce radical sites that intercalate into MMt layers and increase their inter-layers spacing. Subsequently, these radicals on the linear CTS chains initiate the graft-copolymerization of the adsorbed AAm molecules into the clay interlayer spaces, in where the growth of PAAm chains provokes exfoliation of MMt sheets. Then, their crosslinking in presence of the entrapped MMt layers forms the grafted network nanocomposite at x loading of 2 wt.%., 5 wt.%., and 10 wt.%.

C. Characterizations

XRD analysis of pristine MMt, CTS-g-PAAm matrix and its nanocomposites were recorded with a D8 advance diffractometer (Bruker, Inc., Germany) using CuKα monochromatic radiation (40 kV, $\lambda = 1.5406\ A^0$) in $2\theta = 1 - 30°$ with 0.01°/s rate. The surface morphology of these hydrogels was examined on JSM-6360LV Scanning Electron Microscope (JEOL, Inc., USA) using an acceleration voltage of 10 kV.

D. Dye Adsorption Experiments

To study the effects of different experimental parameters, such as, clay content pH and concentration of dye solutions, on the adsorption of MB onto hydrogels nanocomposites, UV spectroscopy was performed on Carry 50 spectrophotometer (Varian, Inc., USA). Batch adsorption experiments were conducted at controlled temperature as follows: a required amount of samples was putted in contact with MB aqueous solution at initial C_0 and was shaken at 200 rpm until reaching adsorption equilibrium. The residual MB was evaluated at 664 nm by analyzing the filtered supernatant and using a previously made calibration curve.

All tests were conducted in triplicate and mean values were considered for fitting process.

The effects of pH and MMt content were studied at 25 °C for 3 h of contact time in MB solution of C0 = 200 mg L^{-1} using 0.1 g L^{-1} of adsorbent dose. Likewise, the adsorbent dose effect was examined in from 0.025 to 0.2 g L^{-1} in C0 of 50 mg L^{-1} for 3 h.

The adsorption capacity at equilibrium (qe, mg g^{-1}) and the removal efficiency R (%) were calculated from (1) and (2), respectively.

$$q_e = \frac{C_0 - C_e}{m} \cdot V \quad (1)$$

$$R(\%) = \frac{C_0 - C_e}{C_0} \times 100 \quad (2)$$

where, C0 and Ce (mg L^{-1}) are dye concentrations at initial and equilibrium times, respectively. V is the volume of dye solution (L), and m is the weight of adsorbent (g).

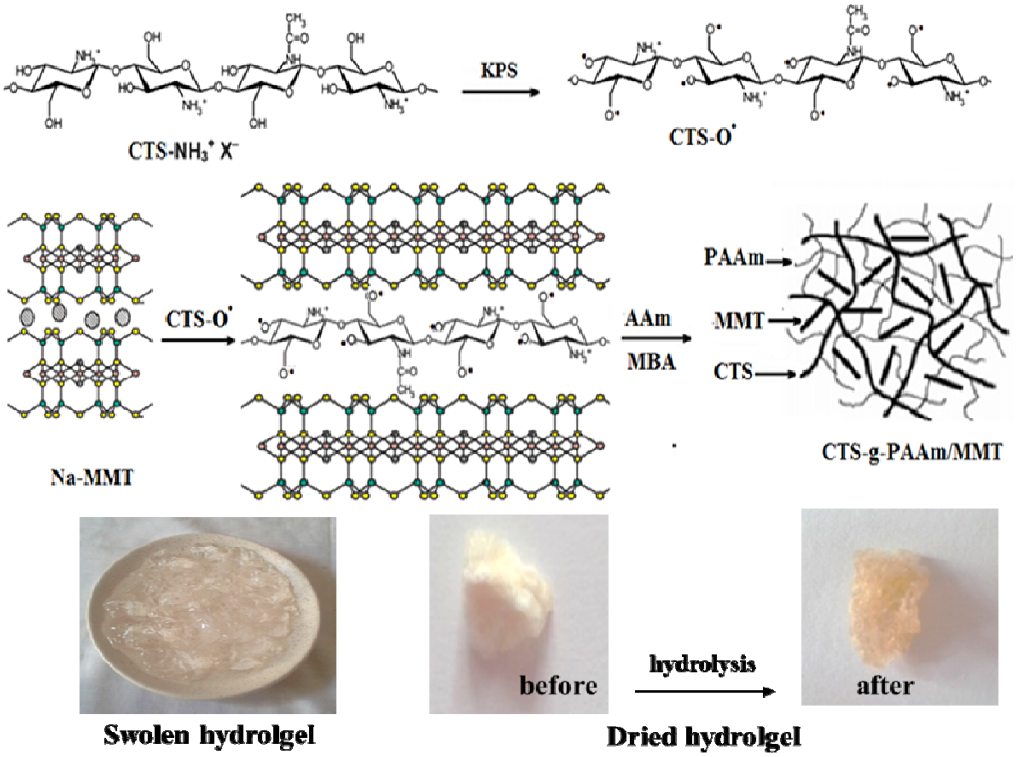

Fig. 1 Mechanism of the formation of grafted CTS-g-PAAm/MMt hydrogel nanocomposites

Kinetics experiments were conducted using 0.1 g L^{-1} of adsorbents in MB solutions of C0 = 200 mg L^{-1} at 25 °C ± 0.2. At desired time intervals, the remaining MB was monitored by taking 2 mL from solution in order to evaluate the amount of MB adsorbed (qt, mg g^{-1}), which was calculated using (1), in where, Ce and qe were replaced with Ct and qt, respectively.

Isotherm adsorption experiments were conducted by varying C_0 in the range of 50 - 800 mg L^{-1} using 0.1 g L^{-1} of each sample for 3 h in neutral pH.

The thermodynamic parameters were evaluated by varying the temperature in the range of 298-318 K using 0.1 g L^{-1} of adsorbent for 3 h for MB C_0 of 200 mg L^{-1} in neutral pH.

E. Regeneration and Reusability Experiments

The indicator for reusability of the developed bioadsorbents is related to their ability to retain good adsorption properties of MB dye molecules after several cycles using a suitable desorption solution. Hence, the regeneration tests of the matrix hydrogel and its representative nanocomposite were conducted in four successive cycles of adsorption/desorption. Typically, adsorption was conducted into 200 mg L^{-1} of MB using 0.1 g L^{-1} of typical adsorbents, at 25 °C.

In desorption process, the MB-loaded samples were shaken in desorbing agent NaCl solution 0.5M of water/ethanol. (50/50 v/v) mixture, then the supernatant was analyzed by UV spectroscopy to calculate the desorbed MB concentration. Concurrently, the regenerated samples were washed with distillated water, and dried for subsequent reuse.

III. Results and Discussion

A. Hydrogel Nanocomposites Characterization

Fig. 2 displays XRD diffractograms of pristine MMt and the elaborated grafted hydrogel matrix CTS-g-PAAm and its MMt-loaded nanocomposites at different contents. As can be seen, the MMt clay exhibits a sharp peak diffraction at 2θ = 6.76° corresponding to basal spacing of the intercalated layers d001 = 1.30 nm. However, this diffraction is not detected for all nanocomposites, no matter how much clay was introduced. This result confirms that MMt platelets are mostly exfoliated and randomly dispersed into the matrix. Indeed, it is well established that in acidic diluted medium the protonated CTS chains rich in NH^{3+} exhibit extend structure that facilitates their intercalation between MMt layers via cationic exchange process. Hence, the occurrence of attractive electrostatic interactions between NH^{3+} groups of CTS and the negatively charges of clay layers surfaces induces substitution of Na+ cations of MMt by CTS chains into interlayers spaces. As

consequence, the nanocomposite is formed via grafting-copolymerization of AAm monomers on CTS backbones, and the subsequent growth of the intercalated PAAm chains induces the exfoliation of clay sheets [12]. These results are similar to studies reported on hydrogels composites based on chitosan-g-poly(acrylic acid)/clays [17], [18].

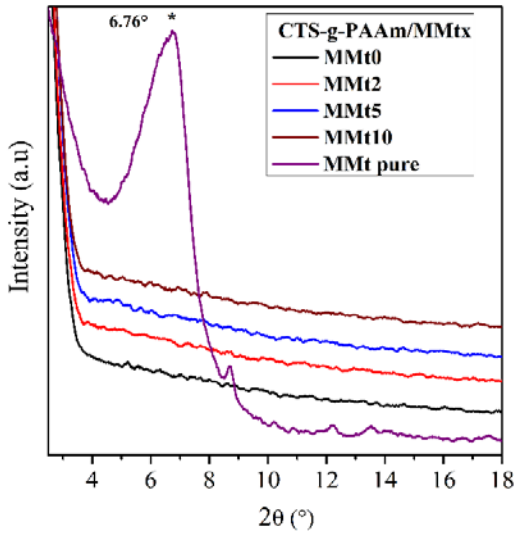

Fig. 2 XRD patterns of pristine MMt, grafted hydrogel matrix and its MMt-loaded nanocomposites

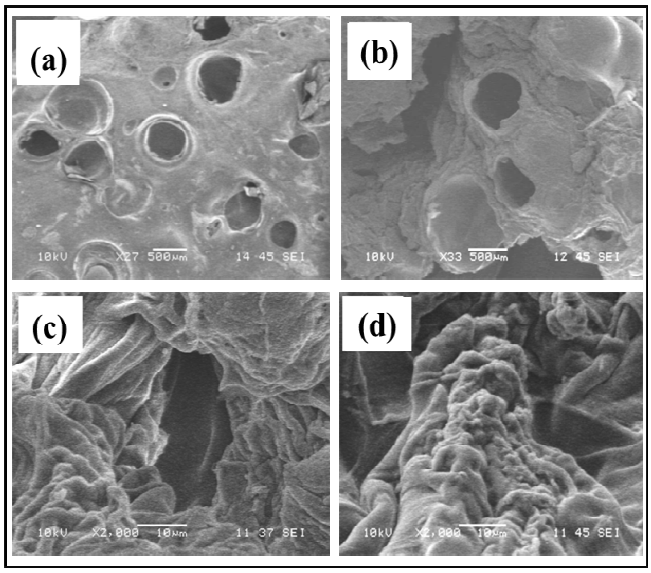

Fig. 3 SEM micrographs of hydrogels surfaces of (a) CTS-g-PAAm matrix and (b-d) its nanocomposites with 2, 5 and 10 wt% of MMt

The surface porosity of hydrogels is the most important characteristic for efficient adsorption capability of pollutants and rate of response by reducing the transport resistance. Figs. 3 (a)-(d) display SEM micrographs of hydrogels surfaces of the matrix CTS-g-PAAm and its nanocomposites, which highlights some changes resulting from the added clay.

Obviously, the nanohybrids surfaces are dissimilar to that of matrix and show more loosely porous, rough, and coarse surfaces. In addition, more gaps are apparent for the highest nanoclay loading. These pores with diameter sizes between 200 nm and 500 nm, are the sites for interaction of external stimuli with the hydrophilic groups of the network and are convenient for the permeation of water, and pollutants of wastewater. Also, homogeneous surfaces are observed, regardless the MMt content, indicating good dispersion of clay within network and thus favorable compatibility between inorganic and organic phases. This finding is in agreement with XRD deductions. Therefore, it is concluded that the incorporation of MMt improves the porous surface of the grafted matrix that is convenient for pollutants adsorption.

B. Factors Influencing MB Adsorption on Hydrogels

MB sorption experiments were performed using a batch method. Stock solution of 1000 mg L^{-1} of MB was prepared in water. Fig. 4 displays MMt loading effect on the equilibrium adsorption capacity (q_e) onto hydrogel matrix and its nanocomposites obtained by varying clay content.

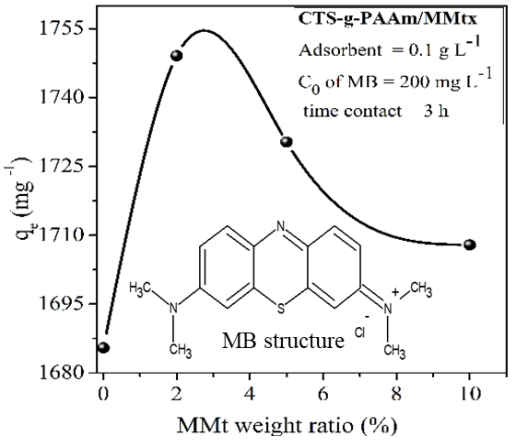

Fig. 4 Effect of MMt content on MB adsorption onto hydrogels (chemical structure of MB dye is shown as insert)

It is clear that the removal capacity is gradually improved by the addition of MMt clay compared to the free-clay matrix and reached an optimum for 2 wt.% of clay. The corresponding maximum q_e value is 1749 mg g^{-1}, which is higher than that of virgin matrix that is 1685 mg g^{-1}. This result highlights the great affinity between adsorbent and MB cationic molecules owing probably to the availability of a higher specific surface area due to the adsorptive properties of layered MMt. Also, the formation of porous structure of hydrogel nanocomposite, as noticed from SEM analysis, enhances the dye adsorption onto the actives sites onto surface and within network pores via mainly electrostatic interactions, supporting the choice of MMt as nanofiller having outstanding adsorbing properties. However, further increase of MMt content beyond the value of 2 wt.% give arise to decrease in adsorption capacity. This fact may be ascribed to the reduction of the available interstitial spaces and pores within the grafted network that become more and more occupy by the embedded MMt particles. In addition, the probable hydrogen bonds establish between the hydroxyls groups on clay layers and

those of matrix increase the crosslinking density, and thus leading to less water and dye penetration. Hence, the nanocomposite prepared with 2% of clay was chosen as the representative adsorbent to further understand the adsorption process.

The influence of adsorbent dose, varying from 0.025 g L^{-1} to 0.2 g L^{-1}, on adsorption capacity and removal efficiency R (%) of MB dye at initial concentration C_0 of 50 mg L^{-1} is illustrated in Fig. 5. Overall, the hydrogels adsorbents display comparable adsorptive behavior: the equilibrium adsorption capacities decrease gradually with increasing their dose, while the corresponding removal values increase up to 0.1g L^{-1} beyond which no significant increase is discerned. As expected, the nanocomposite comprised of 2 wt.% of clay content attained uppermost adsorption data, for which MB removal efficiency increased more speedily with increasing dose. This behavior could be explained by the fact that when the amount of adsorbent is lower, the MB molecules are readily fixed on the active sites. However, more availability of adsorptive sites leads to the decrease of adsorbed dye quantity per gram of adsorbent. Additionally, at higher hydrogel dose, the dye molecules are adsorbed more hardly into the polymer network due to their overlying by the excess of adsorbent, resulting in decrease of surface area per adsorbent particles.

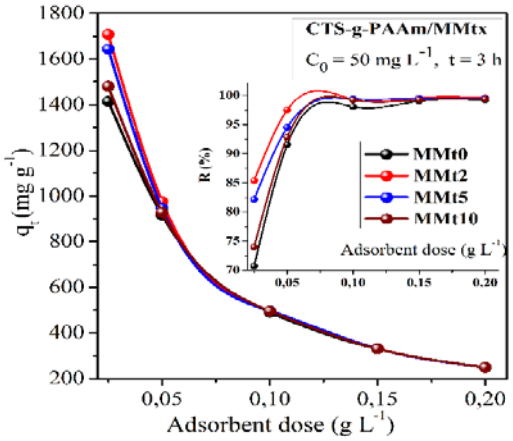

Fig. 5 Effect of hydrogels dose prepared at various MMt contents on MB adsorption

The pH of environment during polluted water treatment is one of the most important parameters affecting the adsorption process since it can affect surface binding sites of adsorbent. So, the effect of the pH ranging from 2 to 12 on the dye adsorption onto hydrogels of matrix and its MMt-loaded nanocomposites is presented in Fig. 4, as shown in Fig. 6. As it can be seen, the equilibrium adsorption capacities of both CTS-g-PAAm and CTS-g-PAAm/MMtx display pH-sensitivity with similar change trend all through the range of pH investigated, suggesting that the added MMt has no influence on the pH-dependence of the matrix. The adsorption was favorable at higher pH since the capacity of all adsorbents increases significantly with increasing pH solutions.

The adsorption capacity for MB dye increased significantly as the pH value approaches 6.0, thereafter become constant until pH 12. The remarkable enhance of dye removal observed at pH > 4 (above pKa) indicates that the most of the carboxylic groups are ionized and interacted with MB molecules. Two probable mechanisms of adsorption process may occur: the main one is through electrostatic interactions between the groups of absorbents (COO^- of matrix, negative charges of MMt layers) and the opposite charged MB dye. The other one is attributes to hydrogen bonding interactions of the reactive hydroxyls groups –OH of clay surface and/or CTS chains with the imines groups –RCH=NR of the MB.

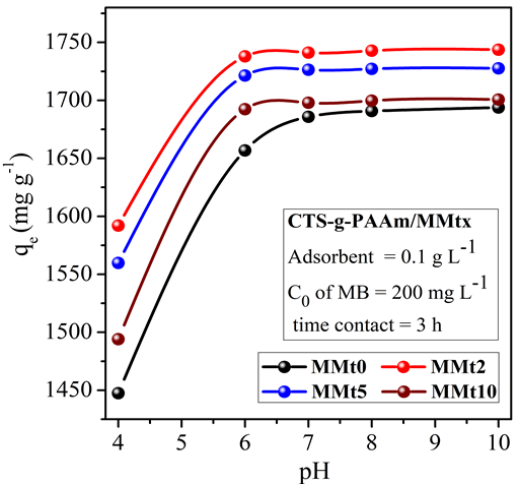

Fig. 6 Effect of pH solution on MB adsorption onto CTS-g-PAAm hydrogels and its MMt-loaded nanocomposites

C. Kinetic Adsorption Studies and Modeling

As the rate of dye adsorption is a crucial factor for proper design of adsorbent, the effect of contact time on MB removal from aqueous solutions is evaluated. Fig. 7 displays the kinetic of MB adsorption onto matrix and its MMt-loaded nanocomposites using 0.1 g L^{-1} in 200 mg L^{-1} of dye aqueous solutions. All adsorbents display significant MB adsorption capacities that increase sharply during 50 min from the initial contact time, where mainly more than 88% of dye removal efficiency (R%) is obtained, and then began to level off until reaching steady state. Indeed, in the initial rapid stage, the molecules dye are adsorbed onto the surface of adsorbents owing to availability of abundant active sites. Upon gradual occupancy of these sites, adsorption became less efficient, so that the molecules gradually diffuse into the pores and are slowly adsorbed by the internal actives sites until reaching equilibrium. In the third stage, the adsorption process is very weak due doubtless to the saturation of ionic actives groups by the MB molecules.

The greater adsorption values are acquired for adsorbents nanocomposites. The incorporation of various contents of clay enhances the adsorption capacity of the matrix CTS-g-PAAm from 1685 mg g^{-1} until an optimum value of 1749 mg g^{-1} reached for nanocomposite containing 2 wt.% of MMt.

To further investigate the adsorption kinetics and evaluate the control factors of adsorption process, the experimental kinetics data were analyzed and simulated using the kinetic

models of pseudo-first-order [19] and pseudo-second-order [20]. The respective equations (3) and (4) give the linear forms of these models.

$$\mathrm{Ln}(q_e - q_t) = \mathrm{Ln}\, q_{e1} - k_1 t \quad (3)$$

$$\frac{1}{q_t} = \frac{1}{k_2\, q_{e2}^2} + \frac{t}{q_{e2}} \quad (4)$$

where q_{1e}, q_{2e}, and q_t (mg.g^{-1}) are the amounts of MB adsorbed (mg g^{-1}) on the adsorbents at the equilibrium and at time t (min), respectively. The parameters k_1 (min^{-1}) and k_2 (g mg^{-1} min^{-1}) are the rate constants of pseudo-first-order and pseudo-second-order models, respectively.

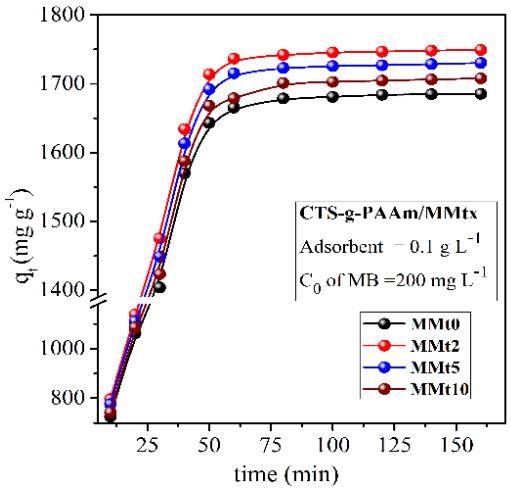

Fig. 7 Curves of time-dependent adsorption of MB at 25 °C onto CTS-g-PAAm hydrogel and its MMt-loaded nanocomposites obtained with different contents of MMt

The plots of ln(qe - qt) versus t and t/qt against t are shown in Fig. 8 and the kinetic parameters are summarized in Table I. From the obtained results, it is noticed that the values of correlation coefficient $R^2 \geq 0.998$ related to pseudo-second-order model are greater than those of pseudo-first-order model for all bioadsorbents and the calculated adsorption capacities at equilibrium (q_{e2}) evaluated by this model are close to the experimental data ($q_{e,\ exp}$). Thus, the pseudo-second-order model adequately describes the MB adsorption onto CTS-based hydrogels. In addition, the values of rate constants (k_2) of all nanocomposites are higher than that of the matrix with a maximum at 2% of MMt content, leading to faster chemical sorption via mainly electrostatic attractions with the cationic dye owed to further anionic sites (negatively charged layers of clay). This result may be also attributed to further porous structure of the nanocomposites networks that promote the diffusion of dye molecules, according to SEM deductions. Similar evolution has been reported for other systems cationic dye/adsorbent [14], [15], [21], [22].

TABLE I
KINETICS PARAMETERS OF MB ADSORPTION ONTO HYDROGELS MMT-LOADED NANOCOMPOSITES AT 25 °C

MMt content (wt.%)	$q_{e,exp}$ mg g^{-1}	Pseudo-premier-order			Pseudo-second-order		
		q_{e1} mg g^{-1}	k_1 min^{-1}	R^2	q_{e2} mg g^{-1}	$k_2.10^4$	R^2
MMt0	1685.4	1919.8	0.102	0.981	1743.98	1.369	0.998
MMt2	1749.1	1370.6	0.117	0.886	1783.17	2.419	0.999
MMt5	1730.3	2844.1	0.129	0.984	1773.05	1.988	0.999
MMt10	1707.9	1324.8	0.075	0.991	1766.78	1.393	0.999

Unit of k_2 is g mg^{-1}min^{-1}

According to the above results, the adsorption mechanism onto composites is proposed in Fig. 9. It is suggested that come non-covalent interactions, e.g., electrostatic interactions and hydrogen bonding, contribute to the adsorption when they act synergistically, and the sorption was much stronger than that driven by the same interactions acting individually. Indeed, the available carboxylate groups on the crosslinked PAAm chains and the negatives charges present on surface and into MMt layers developed ionic interactions with the quaternary ammonium groups of MB molecules. In addition, the presence of hydroxyl OH and amino NH_2 groups on CTS could be implicated in the removal of dye through hydrogen bonding with the amino and/or imines groups of dye. Moreover, the adding of MMt into the grafted hydrogel matrix can effectively improve the adsorption through hydrogen-bond interactions involving their hydroxyl groups.

D.Isotherm Adsorption Studies and Modeling

Adsorption isotherms get their beneficial use from their applicability to identify the interaction between the adsorbent materials and adsorbate of a given system. The effect of varying the initial concentration of MB from 50 mg L^{-1} to 800 mg L^{-1} on adsorption capacity at equilibrium ($q_{e,\ exp}$) of all adsorbents, used at the dosage of 0.1 g L-1 is illustrated in Fig. 10 and the maximum values are regrouped in Table II. Fig. 10 shows also the photographs before and after adsorption.

It is noticed that the values of adsorption capacity of adsorbents increase with increasing concentration of MB until reaching an equilibrium state. This result is ascribed to driving forces during increasing C_0 generated by the gradient of pressure into adsorbents, and hence rising adsorbing affinity to dye molecules [14], [15], [23]. At highest C_0, the actives sites became wholly unavailable since dye molecules crowd them. Also, the aggregation of MB molecules at higher concentration delays their diffusion within hydrogel structure. The values of $q_{e,\ exp}$ and the associated R (%) increased by adding MMt into hydrogel matrix. The maximum $q_{e,\ exp}$ value is reached for the nanocomposite having 2% of clay, denoted MMt2, being 2210.3 mg g^{-1}.

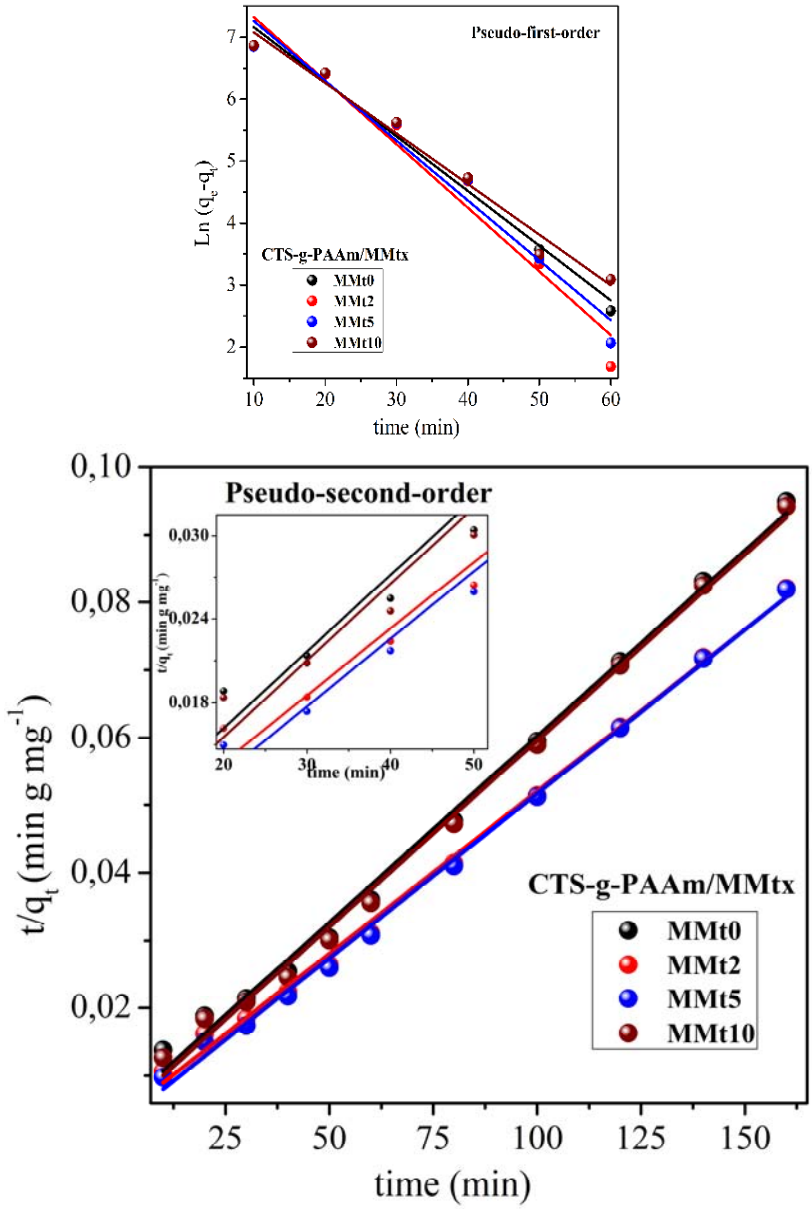

Fig. 8 Kinetics of MB adsorption onto bioadsorbents hydrogels according to (a) pseudo-first-order, (b) pseudo-second-order kinetics

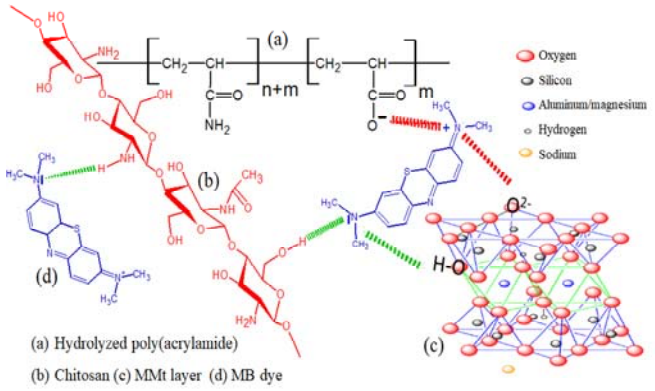

Fig. 9 Mechanism proposed for MB adsorption onto MMt-loaded CTS-g-PAAm hydrogels nanocomposites

Several models can be applied to provide information about the adsorption mechanism as well as the adsorbent surface properties and affinities. The most accepted isotherms models for single solute systems are Freundlich [24] and Langmuir [25] models. Equations (5) and (6) express the respective linear forms.

$$\text{Ln } q_e = \text{Ln } K_F + \frac{1}{n} \text{Ln } C_e \quad (5)$$

$$\frac{C_e}{q_e} = \frac{C_e}{q_m} + \frac{1}{q_m K_L} \quad (6)$$

where, K_F is the Freundlich constant and 1/n is the surface heterogeneity factor (more heterogeneous if it is closer to zero, (1/n) < 1 or > 1 indicates an adsorption process chemically or

physically driven, respectively). K_L is Langmuir constant indicating the affinity of pollutant for binding centers on adsorbents, and the q_m is Langmuir maximum equilibrium adsorption capacity (mg g^{-1}).

The dimensional factor (R_L) from Langmuir model predicts the favorability of adsorption process, favorable ($0 < R_L < 1$), unfavorable ($R_L > 1$), linear ($R_L = 1$) or irreversible ($R_L = 0$) adsorption process. R_L is defined as follows:

$$R_L = \frac{1}{1 + K_L C_0} \quad (7)$$

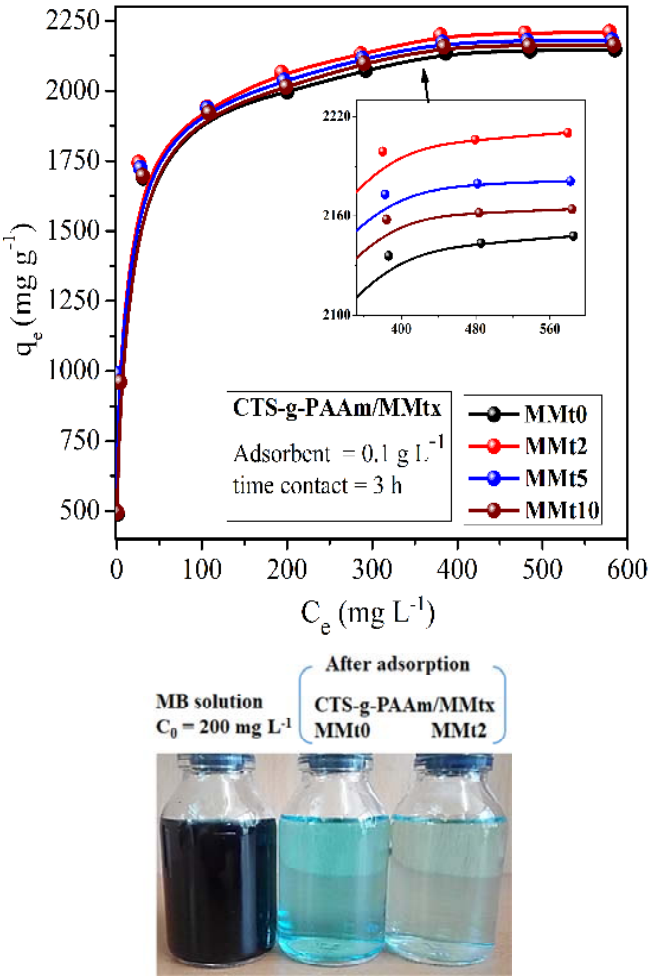

Fig. 10 Isotherms of MB adsorption onto CTS-g-PAAm hydrogel and its MMt-loaded nanocomposites and the photographs of MB solution before and after adsorption

Therefore, the experimental isotherm data of MB adsorption onto these adsorbents are modeled by these equations. Fig. 11 displays the related linear plots and Table II regroups the related isotherm parameters, their correlation coefficients, together with the values of R_L and the experimental data.

The MB adsorption onto adsorbents is well described by the Langmuir model than the Freundlich one since the coefficients R_2 values are the highest and the maximum adsorption capacity calculated from the Langmuir model (q_m) are close to $q_{e,\ exp}$ ones. This result evidences the homogeneity of this process via monolayer adsorption on adsorbents surface. In addition, the R_L values are less than 0.13, confirming the favorability of this process. It is noteworthy that the Langmuir q_m values are increased from 2173.9 mg g^{-1} to 2221.2 mg g^{-1} by adding only 2 wt% of MMt into the matrix. Therefore, the hydrogel nanocomposites display outstanding adsorptive capacities, and hence, could serve as potentially eco-friendly adsorbents for efficient cationic dyes removal from wastewater.

TABLE II
FREUNDLICH AND LANGMUIR ISOTHERM PARAMETERS OF MB ADSORPTION ONTO HYDROGELS NANOCOMPOSITES AT 25 °C

MMt content (wt.%)	$q_{e,exp}$ mg g^{-1}	Freundlich model			Langmuir model			
		K_F 10^{-2} L g^{-1}	n $g.L^{-1}$	R^2	q_m mg g^{-1}	K_L L mg^{-1}	R^2	RR_L[a]
MMt0	2147.7	7.10	5.29	0.867	2173.9	0.10	0.998	0.28
MMt2	2210.3	7.93	5.65	0.915	2221.2	0.21	0.999	0.15
MMt5	2181.1	8.00	5.81	0.918	2192.5	0.25	0.999	0.13
MMt10	2164.1	6.92	5.10	0.951	2193.4	0.11	0.999	0.27

A. Determination of Thermodynamic Parameters

The temperature effect on dye adsorption onto hydrogels adsorbents was studied from 298 K to 318 K. Then, the standard thermodynamic parameters, Gibbs free energy ΔG° (kJ mol^{-1}), enthalpy ΔH° (kJ mol^{-1}), and entropy ΔS° (J mol^{-1} K^{-1}) are evaluated according to (8) and (9):

$$\Delta G° = -RT \ln K_d \quad (8)$$

$$\ln K_d = -\frac{\Delta H°}{RT} - \frac{\Delta S°}{R} \quad (9)$$

where K_d is the ratio of MB quantities at equilibrium state (q_e) to the remaining (C_e). R is the universal gas constant (8.314 J mol^{-1} K^{-1}). Fig. 12 displays lined plots of ln K_d versus (1/T). It is also noticed that the removal efficiency R (%), shown as an insert, increases gradually with rising temperature, indicating a favorable adsorption of MB onto adsorbents. Table III regroups the thermodynamic parameters.

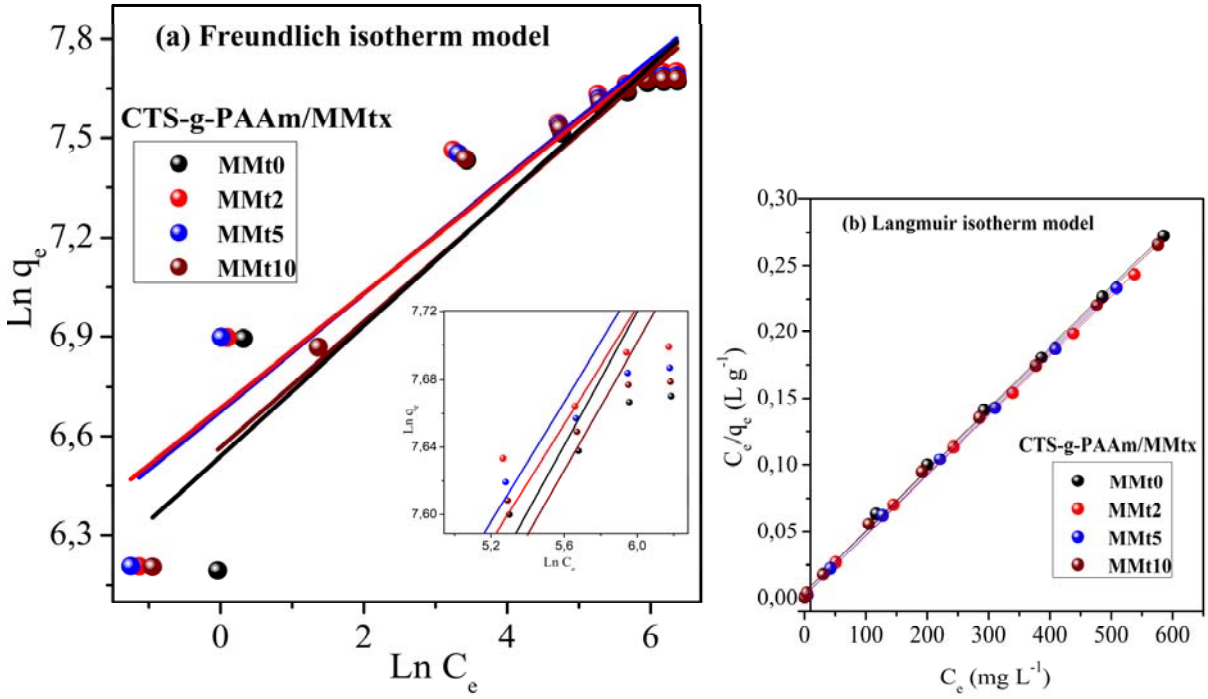

Fig. 11 Linear plots of experimental data according to Freundlich and Langmuir isotherms models

The obtained negative ΔG° values indicate a spontaneous process, while the positive values of ΔH° disclose an endothermic nature. In addition, the ΔH° value ~ 7-8 KJ mol^{-1} confirms the occurrence of a physisorption process [26]. The positive ΔS° reveals randomness at solid/solution interface.

TABLE III
THERMODYNAMIC PARAMETERS FOR THE ADSORPTION OF MB ONTO CTS-BASED HYDROGELS NANOCOMPOSITES

MMt (wt.%)	ΔG_0 (kJ mol^{-1}) at T(K)			ΔH_0 (kJ mol^{-1})	ΔS_0 (J mol^{-1} K^{-1})
	298	308	318		
MMt0	-4.20	-4.63	-5.14	8.24	43.55
MMt2	-4.74	-5.16	-5.80	7.18	39.34
MMt5	-4.54	-4.91	-5.50	7.51	39.54
MMt10	-4.27	-4.66	-5.14	7.46	39.16

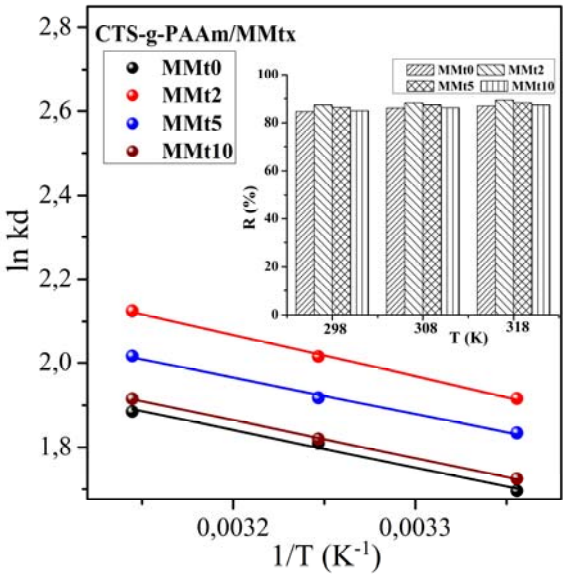

Fig. 12 Influence of temperature on the removal of MB using CTS-g-PAAm hydrogel and MMt-loaded nanocomposites adsorbents

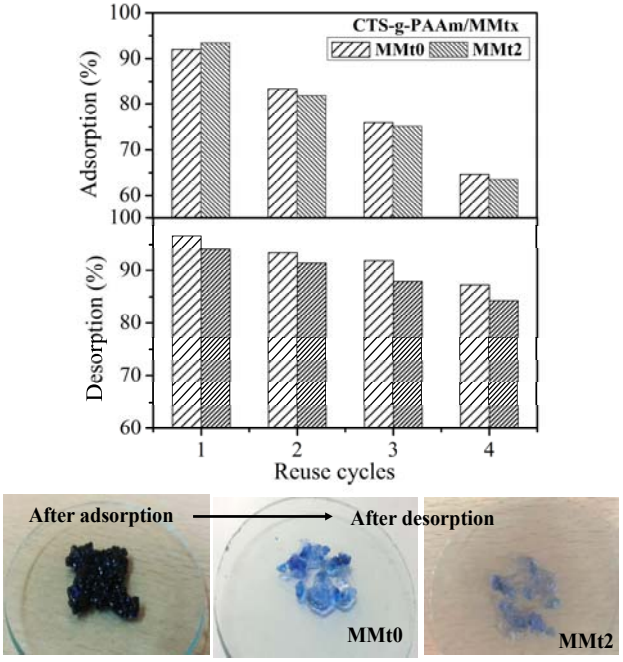

Fig. 13 Performance of CTS-based hydrogels for four cycles of regeneration and photography after adsorption and desorption

B. Regeneration Studies

An outstanding adsorbent must regenerate to reduce the wastewater treatment cost. Moreover, desorption of adsorbed dye can be considered as an important way to reuse adsorbents. Accordingly, the reusability of the hydrogel matrix and its MMt-loaded nanocomposite was conducted at C_0 of 200 mg L^{-1} during four adsorption/desorption cycles, where desorption was accomplished in 0.5M NaCl water/ethanol (50/50 v/v) solution. The result shows effective desorption of MB dye with percentages higher than 84%, which indicates excellent aptitude of the desorbing agent used. The adsorption capacities of the regenerated adsorbents decrease as compared with the starting free-MB hydrogels counterparts but still exhibiting appreciable removal capacity and retain more than 60% of initial activity after four cycles. So, these hydrogels highlight their potential as efficient bioadsorbents for cationic dyes removal from contaminated water.

IV. Conclusion

In this work, eco-friendly bio-adsorbents based on CTS hydrogel nanocomposites have been synthesized and used as adsorbents for the removal of MB from aqueous solutions. The effects of parameters influencing adsorption process such as MMt content, pH of dye solution, contact time, initial concentration of dye solution, temperature were investigated. The results showed that the adsorption capacity for dye increased with increasing pH, contact time and initial dye concentration, but decreased with increasing temperature. These obtained data unveil that all CTS-based hydrogels nanocomposites showed better performance in dye removal as compared to the virgin matrix. By introducing 2 wt.% of clay into the obtained hydrogel nanocomposite showed the highest adsorption capacity and then could be regarded as a potential adsorbent for cationic dye removal from wastewater. The experimental data correlated with the pseudo-second-order kinetic model. Langmuir isotherm was found to be the best model fitting the isotherm adsorption process with maximum capacity of adsorption of 2210 mg g^{-1} for 2% of MMt. The spontaneity and the endothermic nature of the adsorption process were confirmed from thermodynamics parameters.

The adsorbent could be reused with quantitative recovery for four adsorption/desorption cycles. Thus, these sustainable hydrogel nanocomposites with high adsorption capacity are promising bio-based bioadsorbents for efficient recovery of cationic dyes pollutants in wastewater treatments.

References

[1] V. Katheresan, J. Kansedo, S.Y. Lau, "Efficiency of various recent wastewater dye removal methods: A review", *J. Environ. Chem. Eng.*, vol. 6, pp. 4676–4697, 2018.

[2] W. Yang, J. Wang, Q. Yang, H. Pei, N. Hu, Y. Suo, Z. Li, D. Zhang, J. Wang, "Facile fabrication of robust MOF membranes on cloth via a CMC macromolecule bridge for highly efficient Pb(II) removal, *Chem. Eng. J.*, vol. 339, pp. 230–239, 2018.

[3] P. Kumar, A. Pournara, K.H. Kim, V. Bansal, S. Rapti, M.J. Manos, "Metal-organic frameworks: challenges and opportunities for ion-exchange/sorption applications", *Prog. Mater. Sci.*, vol. 86, 25–74, 2017.

[4] M.T. Yagub, T.K. Sen, S. Afroze, H.M. Ang, "Dye and its removal from aqueous solution by adsorption: A review", Adv. *Colloid Interface Sci*., vol. 209, pp. 172–184, 2014.

[5] S. Shakoor, A. Nasar, "Removal of methylene blue dye from artificially contaminated water using citrus limetta peel waste as a very low cost adsorbent", *J. Taiwan Inst. Chem. Eng*., vol. 66, 154–163, 2016.

[6] M.K. Uddin, "A review on the adsorption of heavy metals by clay minerals, with special focus on the past decade", *Chem. Eng. J.*, vol. 308, pp. 438–462, 2017.

[7] H. Ferfera-Harrar, N. Aiouaz, N. Dairi, "Synthesis and Properties of Chitosan-Graft-Polyacrylamide/Gelatin Superabsorbent Composites for Wastewater Purification", *World Academy of Science, Engineering and Technology Inter. J. Chem., Molecular Nuclear Mater. Metallurgical Eng.*, vol.9, pp.757–764, 2015.

[8] N.S. V Capanema, A.A.P. Mansur, H.S. Mansur, A.C. de Jesus, S.M. Carvalho, P. Chagas, L.C. de Oliveira, "Eco-friendly and biocompatible cross-linked carboxymethylcellulose hydrogels as adsorbents for the removal of organic dye pollutants for environmental applications", *Environ. Technol*., vol. 39, pp. 2856–2872, 2018.

[9] H. Ferfera-Harrar, D. Berdous, T. Benhalima, "Hydrogel nanocomposites based on chitosan-g-polyacrylamide and silver nanoparticles synthesized using Curcuma longa for antibacterial applications", *Polym. Bull.*, vol. 75, pp. 2819–2846, 2018.

[10] H. Ferfera-Harrar, N. Aouaz, N. Dairi, "Environmental-sensitive chitosan-g-polyacrylamide/carboxymethylcellulose superabsorbent composites for wastewater purification I: synthesis and properties", *Polym. Bull*., vol. 73, pp. 815–840, 2016.

[11] T. Benhalima, S. Mounsi, N. Dairi, H. Ferfera-Harrar, "Chitosan-g-poly(acrylamide)/Diatomite superabsorbent composites: synthesis and investigation of swelling properties", *Journal of Materials, Processes and Environment*, vol. 4, pp. 21-25, 2016.

[12] H. Ferfera-Harrar, N. Aiouaz, N. Dairi, A.S. Hadj-Hamou, "Preparation of chitosan-g-poly(acrylamide)/montmorillonite superabsorbent polymer composites: Studies on swelling, thermal, and antibacterial properties", *J. Appl. Polym. Sci*., vol. 131, pp.39747.

[13] T. Benhalima, D. Lerari, H. Ferfera-Harrar, "Preparation of carboxymethylcellulose-based hydrogel beads and their used as bioadsorbent of dye from aqueous solutions". *Journal of Materials, Processes and Environment*, vol. 4, pp.113-118, 2016.

[14] T. Benhalima, H. Ferfera-Harrar, D. Lerari, "Optimization of carboxymethyl cellulose hydrogels beads generated by an anionic surfactant micelle templating for cationic dye uptake: Swelling, sorption and reusability studies", *Int. J. Biol. Macromol*., vol. 105, pp. 1025-1042, 2017.

[15] T. Benhalima, H. Ferfera-Harrar, "Eco-friendly porous carboxymethyl cellulose/dextran sulfate composite beads as reusable and efficient adsorbents of cationic dye methylene blue", *Int. J. Biol. Macromol*., vol. 132, pp. 126-141, 2019.
[16] H. Ferfera-Harrar, N. Dairi, "Elaboration of cellulose acetate nanobiocomposites using acidified gelatin-montmorillonite as nanofiller: Morphology, properties, and biodegradation studies", *Polym. Composite*, vol. 34, pp.1515–1524, 2013.
[17] Y. T. Xie, A. Q. Wang, "Preparation and Swelling Behaviour of Chitosan-g-poly(acrylic acid)/Muscovite Superabsorbent Composites"; *Iran. Polym. J*., vol. 19, pp. 131-141, 2010.
[18] J. Zhang, Q. Wang, A. Wang, "Synthesis and characterization of chitosan-g-poly(acrylicacid)/attapulgite superabsorbent composites", *Carbohyd. Polym*., vol. 68, pp. 367-374, 2007.
[19] S. K. Lagergren, "About the theory of so-called adsorption of soluble substances", *Sven Vetenskapsakad Handingarl*., vol. 24 pp.1–39, (1898).
[20] Y.S. Ho, G. Mckay, "Pseudo-second order model for sorption processes", *Process Biochem*., vol. 34, pp. 451-465, 1999.
[21] R.R. Pawar, Lalhmunsiama, P. Gupta, S.Y. Sawant, B. Shahmoradi, S.M. Lee, Porous synthetic hectorite clay-alginate composite beads for effective adsorption of methylene blue dye from aqueous solution., *Int. J. Biol. Macromol*., vol. 114, pp.1315–1324, 2018.
[22] M. V. Nagarpita, P. Roy, S. B. Shruthi, "Synthesis and swelling characteristics of chitosan and CMC grafted sodium acrylate-co-acrylamide using modified nanoclay and examining its efficacy for removal of dyes", *Int. J. Biol. Macromol*., vol. 102, pp. 1226-1240, 2017.
[23] S. Han, T. Wang, B. Li, "Preparation of a hydroxyethyl-titanium dioxide-carboxymethyl cellulose hydrogel cage and its effect on the removal of methylene blue", *J. Appl. Polym. Sci*. vol. 134, pp.44925, 2017.
[24] H.M. F. "Freundlich, Uber die adsorption in losungen", *Z. Phys. Chem*., vol. 57, pp. 385–470, 1906.
[25] I. Langmuir, "The adsorption of gases on plane surface of glass, Mica and Platinum", *J. Am. Chem. Soc*., vol. 40, pp. 1361–1403, 1918.
[26] S. Dawood, T.K. Sen, "Removal of anionic dye Congo red from aqueous solution by raw pine and acid-treated pine cone powder as adsorbent: equilibrium, thermodynamic, kinetics, mechanism and process design", *Water Res*., vol. 46, pp.1933–1946, 2012.